STEM CELLS®

CANCER STEM CELLS

Targeting p90 Ribosomal S6 Kinase Eliminates Tumor-Initiating Cells by Inactivating Y-Box Binding Protein-1 in Triple-Negative Breast Cancers

ANNA L. STRATFORD,[a] KRISTEN REIPAS,[a] KAIJI HU,[a] ABBAS FOTOVATI,[a] RACHEL BROUGH,[b,c] JESSICA FRANKUM,[c] MANDEEP TAKHAR,[a] PETER WATSON,[d] ALAN ASHWORTH,[b,c] CHRISTOPHER J. LORD,[c] ANNETTE LASHAM,[e] CRISTIN G. PRINT,[e] SANDRA E. DUNN[a]

[a]Department of Pediatrics, University of British Columbia, Vancouver, British Columbia, Canada; [b]The Cancer Research UK Gene Function Laboratory; [c]Breakthrough Breast Cancer Research Centre, Division of Breast Cancer Research, The Institute of Cancer Research, London, United Kingdom; [d]BC Cancer Agency, Vancouver Island Cancer Centre, Victoria, British Columbia, Canada; [e]Department of Molecular Medicine and Pathology, School of Medical Sciences, University of Auckland, Auckland, New Zealand

Key Words. Ribosomal S6 kinase • Y-box binding protein-1 • Tumor-initiating cells • CD44 • Therapeutic target

ABSTRACT

Y-box binding protein-1 (YB-1) is the first reported oncogenic transcription factor to induce the tumor-initiating cell (TIC) surface marker CD44 in triple-negative breast cancer (TNBC) cells. In order for CD44 to be induced, YB-1 must be phosphorylated at S102 by p90 ribosomal S6 kinase (RSK). We therefore questioned whether RSK might be a tractable molecular target to eliminate TICs. In support of this idea, injection of MDA-MB-231 cells expressing Flag-YB-1 into mice increased tumor growth as well as enhanced CD44 expression. Despite enrichment for TICs, these cells were sensitive to RSK inhibition when treated ex vivo with BI-D1870. Targeting RSK2 with small interfering RNA (siRNA) or small molecule RSK kinase inhibitors (SL0101 and BI-D1870) blocked TNBC monolayer cell growth by ~100%. In a diverse panel of breast tumor cell line models RSK2 siRNA predominantly targeted models of TNBC. RSK2 inhibition decreased *CD44* promoter activity, CD44 mRNA, protein expression, and mammosphere formation. $CD44^+$ cells had higher P-$RSK^{S221/227}$, P-$YB\text{-}1^{S102}$, and mitotic activity relative to $CD44^-$ cells. Importantly, RSK2 inhibition specifically suppressed the growth of TICs and triggered cell death. Moreover, silencing RSK2 delayed tumor initiation in mice. In patients, RSK2 mRNA was associated with poor disease-free survival in a cohort of 244 women with breast cancer that had not received adjuvant treatment, and its expression was highest in the basal-like breast cancer subtype. Taking this further, we report that P-$RSK^{S221/227}$ is present in primary TNBCs and correlates with P-$YB\text{-}1^{S102}$ as well as CD44. In conclusion, RSK2 inhibition provides a novel therapeutic avenue for TNBC and holds the promise of eliminating TICs. STEM CELLS *2012;30:1338–1348*

Disclosure of potential conflicts of interest is found at the end of this article.

INTRODUCTION

The treatment of triple-negative breast cancer (TNBC) suffers from the lack of targeted therapies. Unlike estrogen receptor (ER)-positive or HER-2-positive breast cancers, which can be treated with anti-estrogens and Herceptin, respectively, treatment options rest entirely upon conventional chemotherapies. While these tumors often initially respond very well to chemotherapy, they commonly become resistant in the long-term leading to relapse [1, 2]. Tumor-initiating cells (TICs), which are $CD44^+/CD24^-$, are more frequent in TNBC than other breast cancer subtypes [3–6] and have been linked to tumor recurrence. This is, in part, due to the fact that they are intrinsically resistant to traditional chemotherapy and radiotherapy [7–9], but also the percentage of TICs increases following chemotherapy [7, 10]. The loss of CD44 also suppresses mammosphere formation [11], growth, and branching morphogenesis [11]. Thus, identifying targeted therapies that are able to uniquely eliminate TICs, as well as the bulk of the tumor, is critical [12] as they are the most likely to improve TNBC patient outcome.

Author contributions: A.L.S. and K.R.: conception and design, collection and/or assembly of data, data analysis and interpretation, and manuscript writing; K.H. and R.B.: collection and/or assembly of data and data analysis; A.F.: collection and/or assembly of data, data analysis, and manuscript writing; J.F. and M.T.: collection and/or assembly of data; C.J.L. and A.A.: data analysis and study design; P.W.: provision of study material or patient; A.L.: data analysis; C.G.P.: provision of study material or patient and collection and/or assembly of data; S.E.D.: conception and design, data analysis and interpretation, manuscript writing, and final approval of manuscript. A.L.S. and K.R. contributed equally to this article.

Correspondence: Sandra E. Dunn, Ph.D., Experimental Medicine Program, University of British Columbia, 950 W. 28 Ave, Vancouver, British Columbia V5Z 4H4, Canada. Telephone: 604-875-2000, ext. 6015; Fax: 604-875-3120; e-mail: sedunn@mail.ubc.ca Received January 23, 2012; accepted for publication April 27, 2012; first published online in STEM CELLS *EXPRESS* June 4, 2012. 1066-5099/2012/$30.00/0 doi: 10.1002/stem.1128

TICs are characterized as having the ability to self-renew, grow as mammospheres, invade, and initiate tumor formation in mice [12–14]. Using this battery of assays, new inhibitors are being sought to eliminate TICs. Compounds that are effective against both TIC and non-TIC populations within tumors are optimal as they would eliminate the bulk population as well as the drug-resistant TICs. Promising examples include targeting epidermal growth factor receptor (EGFR)/Her-2 with lapatinib or the Notch receptor with gamma secretase inhibitors [8]; however, these leads only provide modest growth suppression. The NFκB [15] and TGFβ [16, 17] pathways are also implicated in TICs based on gene expression analysis of $CD44^+/CD24^-$ cells. Most targeted therapies are directed toward kinases that mediate signal transduction [18]; therefore, perhaps an alternative strategy for targeting individual receptor tyrosine kinases is to suppress a common convergence point farther downstream.

The p90 ribosomal S6 kinase (RSK) family of kinases are activated by receptor tyrosine kinases such as the EGFR, fibroblast growth factor, and insulin-like growth factor receptors that are commonly activated in TNBC [19–22]. This allows RSK to phosphorylate downstream targets involved in tumor growth, invasion, and epithelial-mesenchymal transition [19, 23]. These include transcription factors such as Y-box binding protein-1 (YB-1) [22], creb, and c-fos [24] as well as the anti-apoptosis protein BAD [25], the translation factor GSK3β [26], and histone H3 [27, 28]. More specifically, RSK phosphorylates YB-1 at S102 leading to nuclear translocation and transcriptional activation [22]. Here, YB-1 induces a TIC phenotype by upregulating CD44 and CD49f [11]. Conversely, we have shown that knocking down YB-1 using small interfering RNA (siRNA) suppresses CD44 expression and mammosphere formation [11]. Of clinical relevance, RSK is also activated by commonly used chemotherapies such as paclitaxel leading to the phosphorylation of YB-1^{S102} and ultimately to the induction of CD44 [11]. One strategy in the pursuit of TIC ablation is to inhibit P-YB-1^{S102}, which leads to reduced CD44 and TICs; however, this has only been achievable with siRNAs as there are no small molecules available to block YB-1 directly. Therefore, we addressed whether blocking the activation of YB-1 via RSK inhibition could be an alternative approach to combating relapse by eliminating TICs.

Materials and Methods

Cell Lines and Reagents

SUM149 (Asterand, Detroit, MI, www.asterand.com) and MDA-MB-231 (ATCC; Manassas, VA, www.atcc.org) cells were used as models of TNBC and cultured as previously described [22]. For high-throughput cell-based screening, breast tumor cells lines were purchased from either Asterand or ATCC and maintained according to the distributor's instructions. 184htert, immortalized normal breast epithelial cells, were cultured as previously described [29]. RSK-specific inhibitors SL0101 (Toronto Research Chemicals Inc., North York, ON, Canada, www.trc-canada.com) was dissolved in methanol [30], and BI-D1870, a kind gift from Dr. Ching-Shih Chen, was dissolved in dimethyl sulphoxide (DMSO). RSK1 and RSK2 siRNA were obtained from Qiagen (Mississauga, ON, Canada, www.qiagen.com).

siRNA Transfections

Cells were transfected with siRNA (20 nM) (Qiagen) with RNAiMAX (Invitrogen, Burlington, ON, Canada, www.invitrogen.com.) using the fast forward protocol. All experiments were performed once the cells had been transfected for 72 hours unless otherwise stated.

RNAi Screening

Breast tumor cell line models were siRNA screened as described in [31], using Cell Titer Glo reagent (Promega, Madison, WI. www.promega.com) to estimate cell survival after five population doublings. For further details see Supporting Information Methods.

Semiquantitative Real-Time PCR

RNA was extracted from cells and xenograft tissue (RNeasy mini kit; Qiagen) and converted into cDNA (superscript III; Invitrogen). Quantitative real-time PCR (qRT-PCR) was performed to detect CD44, RSK1, RSK2, and 18s ribosomal subunit using Taqman gene expression assays (Applied Biosystems, Carlsbad, CA, www.appliedbiosystems.com).

Western Blot Analysis

Immunoblotting was performed as previously described [32]. Antibodies were used as listed in Supporting Information Methods.

Mammosphere Assay

Cells were seeded (SUM149: 20,000 cells per well; MDA-MB-231: 10,000 cells per well) in ultra-low adherent six-well plates (StemCell Technologies, Inc., Vancouver, BC, Canada, www.stemcell.com) and grown in MammoCult (StemCell Technologies) supplemented with hydrocortisone and heparin. Spheres were counted after 7 days. For post-treatment of established spheres, BI-D1870 was added in fresh media to wells after 72 hours.

Growth and Apoptosis Assays

Cells were seeded (3,000–5,000 cells per well) in 96-well plates, treated with inhibitors or siRNA, and allowed to grow for a further 72 hours—10 days (siRNA refreshed every 3 days). Cells were stained as previously described [21]. Apoptosis was measured by propidium iodide (PI) uptake, P-H2AX^{S139} staining, and PARP and Caspase-3 cleavage. For further details see Supporting Information Methods.

Clonogenic Assay

SUM149 cells were seeded in a six-well plate (4×10^5 cells per well) and treated with DMSO or BI-D1870 (10 μM) for 72 hours. Surviving cells were counted and reseeded in six-well plates (1,000 cells per well). After 7 days, clonal colonies were visualized with crystal violet and manually counted.

CD44 Promoter Assay

SUM149 cells were transfected with a CD44 promoter construct, as previously described [11]. Cells were treated with BI-D1870 (10 μM) 6 hours prior to harvest.

Immunofluorescence

Staining for nuclear localization of P-YB-1^{S102} and P-histone $H3^{S10}$ was performed using SUM149 (5,000 cells per well) seeded in a 96-well plate and treated with BI-D1870 at 24 hours then allowed to grow for a further 48 hours. For details of staining procedure see Supporting Information Methods.

YB-1^{D102} Rescue

SUM149 cells were seeded in six-well plates (4×10^5 cells per well) and transfected 24 hours later with 5 μg 3xflag:EV or 3xflag:YB-1S102D (D102) using FuGene HD (Roche, Laval, QC, Canada, www.roche-applied-science.com). After 24 hours, cells were reseeded in 96-well plates (5,000 cells per well). Remaining cells were collected for protein analysis. Plated cells were treated with BI-D1870 for 72 hours and then stained for Hoechst as described in Supporting Information.

Fluorescence-Activated Cell Sorting Analysis

A single-cell suspension of SUM149 cells was obtained as previously described [11]. Cells were stained with CD44-PE conjugated (BD Pharmingen, Missassauga, ON, Canada, www.bdbiosciences.com), CD24-FITC conjugated (StemCell Technologies), and 7-aminoactinomycin D (7-AAD) viability dye (BD Pharmingen) and sorted for the top 10% $CD44^+/CD24^-$ population.

In Vivo Tumor Growth Xenograft Model

All experimentation involving mice were conducted in accordance with the standard protocol approved by the University Committee on the Use and Care of Animals at the University of British Columbia.

YB-1 Overexpressing Cells

Injections were performed using stable cell lines containing either Flag-YB-1 or control empty vector (EV) in the MDA-MB-231 created as previously described [11]. Cells (500 cells per injection) were resuspended in phosphate buffered saline (PBS) containing 25% matrigel (BD biosciences) and injected into the fourth inguinal mammary gland of 6–8 weeks old female nonobese diabetic/severe combined immunodeficient (NOD/SCID) mice (Charles River). Tumors were measured using a digital caliper and volume was calculated using $V = W^2 \times L/2$.

Effect of RSK2 on Tumor Initiation

To test the effects of transient RSK2 knockdown on tumor initiation, MDA-MB-231 cells were transfected with either RSK2 siRNA or control siRNA for 48 hours. Knockdown was validated using both qRT-PCR and Western blot analysis. Orthotopic mammary fat pad (MFP) injections were performed in a similar manner as described above. In order to achieve tumor initiation at a time that would capture the effects of RSK2 knockdown mice were injected with 1×10^6 cells per injection. A tumor was considered to be anything measuring $r > 2.5$ mm.

Dissociation of Tumors

Mice were humanely euthanized when tumors reached ~500 mm^3. Tumors were harvested, dissociated mechanically, and digested in DMEM containing collagenase/hyaluronidase (StemCell Technologies) at 37°C for 4 hours. Red blood cell lysis was performed by incubating the suspension in ammonium chloride. To ensure a single-cell suspension, the cells were passed through a 40 μM nylon mesh. This was then used to perform flow cytometry, Western blot analysis, and drug treatment experiments.

Flow Analysis

Cultured or xenograft cells were resuspended in fluorescence-activated cell sorting (FACS) buffer (PBS containing 2% FBS and 5 mM EDTA then stained with CD44-PE conjugated (BD Pharmingen), CD24-FITC conjugated (StemCell Technologies), and 7-AAD viability dye (BD Pharmingen). Cells were washed once and resuspended at $\sim 10 \times 10^6$ cells per ml in FACS buffer and collected using a FACS Calibur. Analysis was performed using Flowjo software.

RSK2 Survival and Subtype Analyses

RSK2 mRNA levels were assessed in RMA-normalized Affymetrix HG-U133A or HG-U133PLUS2 microarray data from 771 clinically annotated breast tumors drawn from five breast cancer cohorts as previously described [33]. Using the only probe set for RSK2 (RPS6KA3-203843_at), expression levels were plotted against histological grade and subtype for all 771 patients, followed by one-way analysis of variance and Tukey's Honestly Significant Difference test to determine the statistical significance, using the R statistical environment. In addition Kaplan-Meier survival analysis with both log-rank significance tests [34] (comparing above vs. below RSK2 median expression) and significance tests using Cox proportional hazards models (http://cran.r-project.org/web/packages/survival/) were performed on those 244 patients who had not received any kind of adjuvant treatment. Patients with events ≥12 years were excluded, since more than 82% of these patients came from a single cohort [35].

Immunohistochemistry

A breast cancer TMA of 18 patients with high-grade infiltrating ductal tumors was obtained and stained. The sections were stained with P-YB-1^{S102} (1:100), P-$RSK^{S221/227}$ (1:200), or CD44 (1:100) antibodies. Statistical analyses were performed using JMP version 8.0.2 (SAS Institute Inc). Bivariate correlations between study variables were calculated by Spearman's rank correlation coefficients. Differences were considered statistically significant for p values $<.05$. Scale bars on images represent 100 μm.

RESULTS

RSK Inhibitor BI-D1870 Is Effective at Suppressing Growth of a YB-1-Induced $CD44^+$ Population

We have previously identified YB-1 as an oncogenic transcription factor with the ability to regulate a TIC phenotype including; TIC markers CD44 and CD49f as well as mammosphere formation and drug resistance [11]. Using YB-1 as the driver to induce a CD44-high population, we created stable cell lines expressing a Flag-YB-1 transgene in MDA-MB-231 cells (Fig. 1A). When injected into the mammary fat pad of NOD/SCID mice (500 cells per mammary fat pad), cells overexpressing YB-1 demonstrated a significantly increased growth rate when compared with EV control cells (Fig. 1B). The tumors were isolated and cell lines were established and characterized for TIC markers. We noted that the tumors arising from Flag-YB-1 cells had increased CD44 expression as indicated by immunoblotting (Fig. 1C). A second YB-1 target gene, CD49f was also confirmed to be induced in these explanted cell cultures (Fig. 1C). P-YB-1^{S102} was elevated in the Flag-YB-1 cells, although it is still present in the EV cells (Fig. 1C). The induction of CD44 was further confirmed in a second pair of explanted tumors from MDA-MB-231 cells expressing the EV as compared to Flag-YB-1 (data not shown). Interestingly, despite having an increased $CD44^+$ population, BI-D1870, a small molecule RSK ATP competitive inhibitor, was capable of inhibiting growth in the Flag-YB-1 cell population *ex vivo* suggesting that Flag-YB-1 relies on RSK for enhanced growth (Fig. 1D). In both *ex vivo* cell lines, the target P-YB-1^{S102} was eliminated following treatment with BI-D1870 (Fig. 1D). To further elucidate the role of RSK1 and RSK2 separately on YB-1 activation, an in vitro kinase assay was performed using a YB-1 peptide as the substrate [22, 36]. Both RSK1 and RSK2 directly phosphorylate YB-1 at Ser102, which can be inhibited with BI-D1870 (Supporting Information Fig. S1A). Additionally, BI-D1870 was shown to block activation of a second downstream RSK substrate GSK3β (Supporting Information Fig. S1B). Thus, YB-1 drives tumor initiation *in vivo* and the tumors that arise have higher level of TICs. While CD44 is high in the emergent tumors, they are sensitive to the RSK inhibitor.

RSK2 siRNA Suppresses Growth of TNBC Cells

Next, we asked whether there was a specific RSK isoform that supports the growth of TNBCs. We treated TNBC cell lines SUM149 with RSK siRNAs that led to a >90% loss in their target protein expression after 72 hours (Fig. 2A inset). This corresponded with a similar decrease in P-YB-1^{S102} (Fig. 2A inset). Targeting RSK2 with siRNA every 72 hours for a total period of 10 days inhibited the growth of the TNBC cell

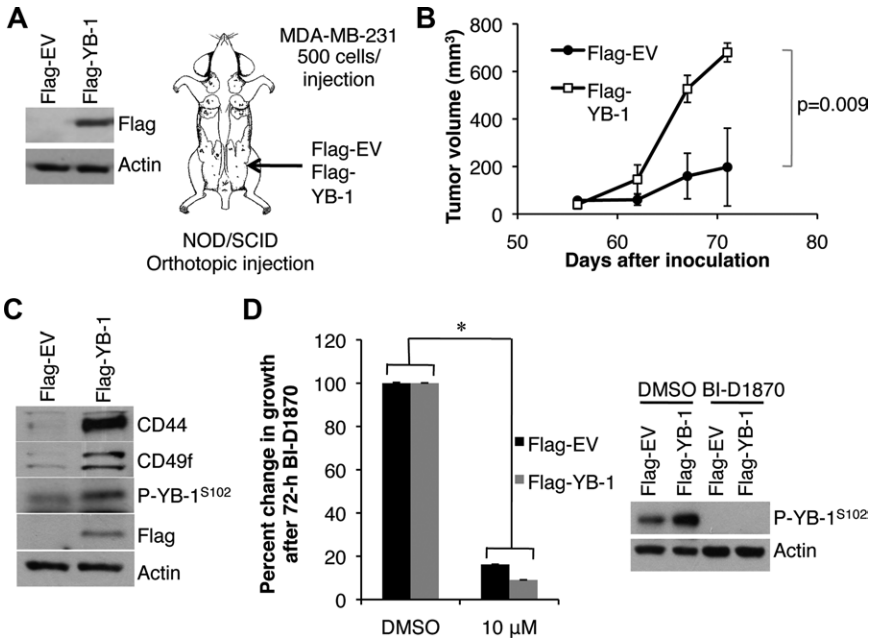

Figure 1. YB-1-induced CD44^{high} cells remain sensitive to RSK inhibition by BI-D1870. **(A):** Stable incorporation of Flag-YB-1 into the MDA-MB-231 cell line was validated by Western blot and 500 cells were injected into the fourth inguinal mammary fat pads of NOD/SCID mice. **(B):** Tumors from cells expressing Flag-YB-1 had significantly increased growth rates compared to EV control tumors. **(C):** Cells isolated from tumors expressing Flag-YB-1 had higher expression of the tumor-initiating cell markers CD44 and CD49f as well as P-YB-1^{S102} as assessed by Western blot. **(D):** RSK inhibition via BI-D1870 (10 μM) suppressed growth and P-YB-1^{S102} in the Flag-YB-1 population with comparable efficacy as in the control EV cells. Control Western blot demonstrates P-YB-1^{S102} suppression by BI-D1870 in both cell lines. Abbreviations: DMSO, dimethyl sulphoxide; EV, empty vector; NOD/SCID, nonobese diabetic/severe combined immunodeficient; YB-1, Y-box binding protein-1. *$p < 0.05$.

line SUM149 by >90% (Fig. 2A). A consistent growth inhibition was observed at 72 hours using two distinct siRNAs against both RSK 1 and 2 (Supporting Information Table S1). RSK2 inhibition was far more effective at suppressing tumor cell growth than RSK1 as loss of the former suppressed growth by almost 100% and the latter by 50% (Fig. 2A). The importance of RSK2 in the growth of TNBC cells was further confirmed in an unbiased screen of siRNAs targeting >700 kinases in 20 breast cancer cell line models representing the major subtypes of the disease [31]. In the primary screen, siRNA targeting RSK2 selectively suppressed the triple-negative models ($p < .05$ permutation t test) and was one of the very limited number of genes that was able to elicit such a TNBC-specific effect (Fig. 2B). This screen result was validated using multiple different siRNAs targeting RSK2 in a panel of 20 genetically diverse cell lines (Supporting Information Fig. S2), where RSK2 siRNAs preferentially inhibited TNBC models but was not particularly effective against non-TNBC cell lines ($p < .002$ TNBC inhibition vs. non-TNBC model inhibition for two different RSK2 siRNA species and $p < .007$ for the RSK2 siRNA pool, t test).

BI-D1870 Blocks the Growth of TNBC Cells

We then sought to determine whether we could achieve similar growth suppression by treating TNBC cell lines with small molecule RSK inhibitors. Inhibiting pan RSK kinase activity with BI-D1870 (2 μM or above) reduced the growth of SUM149 cells by >90% after 10 days, with repeated dosing every 3 days (Fig. 2C). Suppression of P-YB-1^{S102} was confirmed by immunoblotting at 96 hours (Fig. 2C inset). Furthermore, BI-D1870 (0.1–10 μM) or SL0101 (25–100 μM), a second RSK inhibitor, suppressed P-YB-1^{S102} and tumor cell growth by up to >90% after only 72 hours (Supporting Information Fig. S3A and S3B, respectively). To establish that P-YB-1^{S102} was a mediator of the effect observed following treatment with BI-D1870, we transfected SUM149 cells with activated YB-1 (D102) or EV and after 24 hours exposed these cells to BI-D1870 (5 and 10 μM) for 72 hours. Cell growth was then measured, and as expected in the EV-transfected cells, BI-D1870 killed >80% of the cells (Fig. 2D). This phenotype was partially rescued in the D102-transfected cells (50% growth inhibition) (Fig. 2D). Transgene expression was validated by immunoblotting (Fig. 2D inset).

Next, we asked whether the few cells that remain following treatment with BI-D1870 are in fact resistant to the drug. Cells that remained after 72 hours BI-D1870 treatment were plated at low density along with control-treated cells. While the control-treated cells formed colonies in this clonogenic assay, there was 100% growth suppression of the BI-D1870-treated cells, indicating that these cells have not developed resistance to the drug (Fig. 2E). Having demonstrated a growth suppressive effect following RSK inhibition, we then assessed induction of apoptosis. Treating the SUM149 cells with either BI-D1870 or RSK siRNA resulted in the induction of apoptosis. This is demonstrated by PI uptake (Fig. 2F), P-H2AX^{S139} (Supporting Information Fig. S3C), and PARP cleavage (Supporting Information Fig. S3D). Additionally, both SUM149 and MDA-MB-231 cells stained positively for the apoptotic marker Annexin-V when treated with BI-D1870 (1, 5, or 10 μM) for 48–72 hours (Supporting Information Fig. S3E, S3F). Thus, TNBCs are dependent upon RSK signaling to sustain tumor growth.

Inhibiting RSK Decreases CD44 Expression

Keeping in mind that the frequency of TICs is higher in TNBC than in other breast cancer subtypes and that RSK inhibition decreases the growth of TNBC cell lines, we suspected it would also have an effect on TICs. As previously mentioned, TICs are induced by the RSK substrate YB-1 through binding to the CD44 promoter in a phosphorylation-

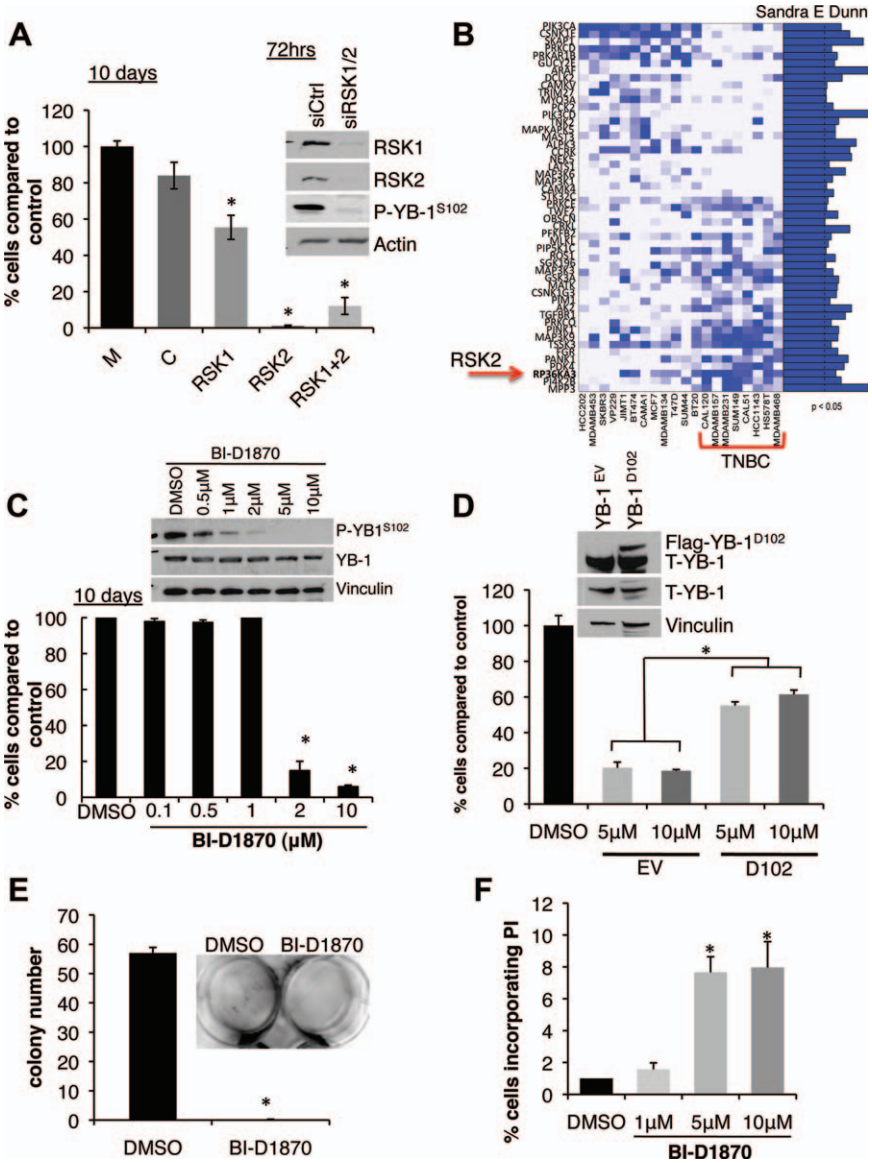

Figure 2. Inhibiting RSK suppresses growth of TNBC cell lines. **(A):** SUM149 cells transfected with small interfering RNA (siRNA) against RSK1 and/or RSK2 for 10 days showed 50%–100% growth suppression. Western blot demonstrates loss of protein after 72 hours. **(B):** Suppression of RSK2 using siRNA in a large kinase screen preferentially decreased the viability of TNBC cell lines as opposed to non-TNBC cell lines. **(C):** Doses of BI-D1870 as low as 2 μM results in 80% reduction of SUM149 cell growth. Western blot demonstrates decreased P-YB1^{S102} across a range of BI-D1870 concentrations at 96 hours. **(D):** The effect of BI-D1870 on SUM149 cell growth could be partially rescued through expression of an activated YB-1 mutant (D102). Transgene expression was validated by Western blot. **(E):** Cells that survived 72-hour BI-D1870 treatment were seeded at low density in the RSK inhibitor and allowed to grow for 10 days. Treated cells did not grow in this clonogenic assay. **(F):** Treatment of SUM149 cells with BI-D1870 resulted in the induction of apoptosis as measured by PI uptake. Abbreviations: DMSO, dimethyl sulphoxide; EV, empty vector; PI, propidium iodide; RSK, ribosomal S6 kinase; TNBC, triple-negative breast cancer; YB-1, Y-box binding protein-1. *$p < 0.05$.

dependent manner [11, 22]. Site-directed mutants that prevent YB-1^{S102} phosphorylation stop nuclear trafficking and override YB-1's ability to induce TICs [11]. BI-D1870 was therefore used as a chemical probe to mirror this effect. BI-D1870 inhibited the nuclear translocation of P-YB-1^{S102} in SUM149 cells (Fig. 3A) and CD44 promoter activity (Fig. 3B). Moreover, decreases in CD44 transcript levels were observed following treatment with RSK1/2 siRNA or BI-D1870 (Fig. 3C and Supporting Information Fig. S4), with a concomitant reduction in the number of cells expressing high levels of CD44 (Fig. 3D). Interestingly, as with the effect on growth, suppression of RSK2 with siRNA resulted in a much larger decrease in CD44 transcript levels than that of RSK1 (Fig. 3C). A fundamental problem with many chemotherapeutic agents is that they induce CD44 expression [7], and this is thought to be involved in drug resistance and recurrence. Herein, we show that treatment of SUM149 cells with paclitaxel-induced CD44 expression, but this was not the case with BI-D1870 (Fig. 3E). More importantly, combining paclitaxel treatment with BI-D1870 reduced the induction of CD44 by the former (Fig. 3E).

Targeting RSK Inhibits TIC Growth

While conducting high content screening, we unexpectantly noticed that CD44^{+} cells were more proliferative than the CD44^{-} cells, having a greater number of mitotic figures based

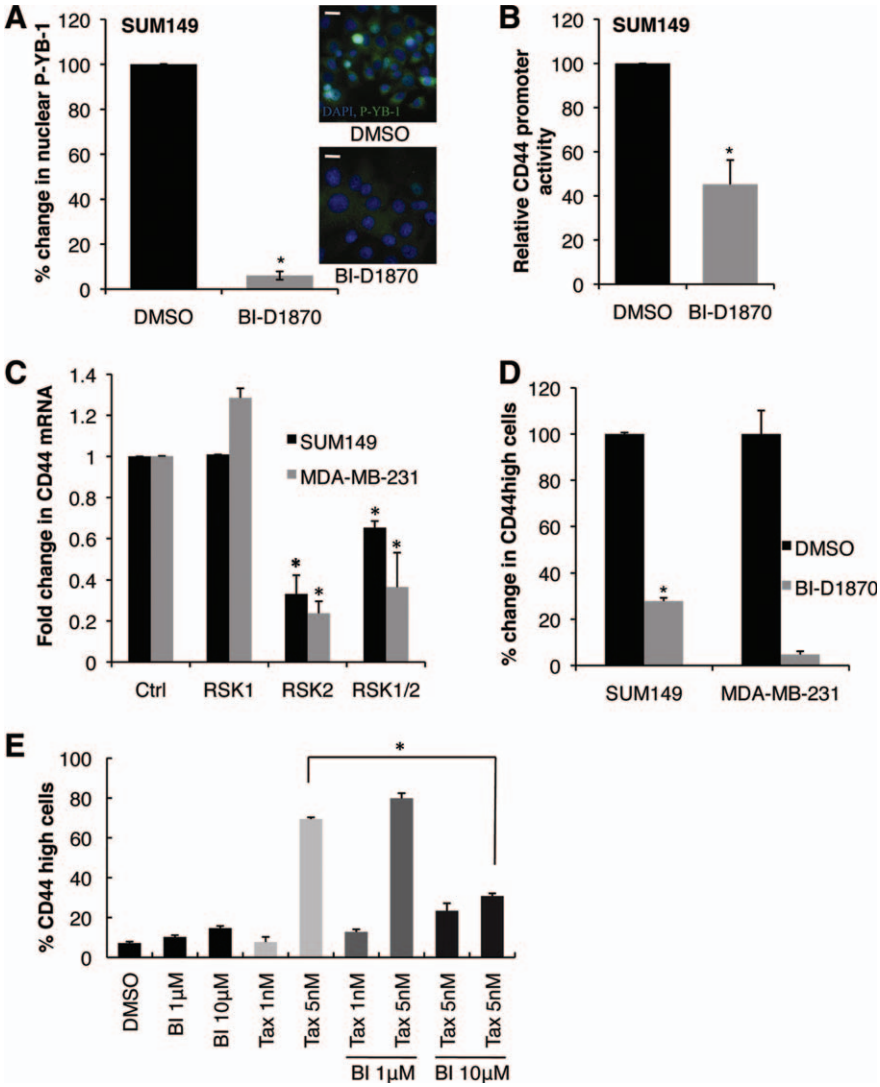

Figure 3. RSK inhibition decreases CD44 expression. **(A):** Treating SUM149 cells with BI-D1870 decreases nuclear localization of P-YB-1^{S102}. Immunofluorescence shows P-YB-1^{S102} (green) and DAPI (blue). Scale bar = 20 μm. **(B):** Inhibiting RSK with BI-D1870 decreases CD44 promoter activity. **(C):** CD44 transcript levels decrease after treatment with RSK siRNA in the SUM149 and MDA-MB-231 cell lines. **(D):** The CD44^{high} fraction in cell populations was reduced upon RSK inhibition with BI-D1870 (10 μM). **(E):** Taxol, but not BI-D1870, induces CD44 expression. Furthermore, the combination of BI-D1870 and Taxol prevented the induction of CD44. Abbreviations: DMSO, dimethyl sulphoxide; RSK, ribosomal S6 kinase; YB-1, Y-box binding protein-1. *$p < 0.05$.

on Hoechst staining (Supporting Information Fig. S5A). To further validate this, we stained for a second marker of mitosis, P-histone H3^{S10}, an early M-phase marker. Consistently, we found that CD44$^+$ cells had higher P-histone H3^{S10} expression and were more actively undergoing mitosis (Fig. 4A). The replicative capacity of CD44$^+$ cells was blunted by exposing the cells to increasing amounts of BI-D1870 (Fig. 4B). There were also fewer CD44$^+$ cells in total (Fig. 4C). As, P-histone H3^{S10} is downstream of RSK signaling, the suppression in growth in the CD44$^+$ population may be in part due to a perturbed mitotic process [27, 28]. Thus, RSK inhibition repressed TICs ability to replicate. Taking this further, we examined the impact of RSK inhibition on mammosphere growth. CD44$^+$ cells have a higher capacity to form mammospheres as compared to CD44$^-$ cells as previously reported by our group and several others [8, 10, 11, 13, 14, 37] and reproduced herein (Supporting Information Fig. S5B). Additionally, it has been shown that knocking down CD44 reduces the ability of cells to form mammospheres [11]. As a functional readout of TICs, we therefore measured the ability of MDA-MB-231 and SUM149 cells to form mammospheres in culture. In line with the decreased CD44, RSK inhibition markedly suppressed mammosphere formation by 80%–100% (Fig. 4D and Supporting Information Fig. S5C). As there was such a substantial effect, it was not possible to serially passage the spheres. Furthermore, the compound caused regression of established mammospheres (Fig. 4E).

Next, TICs (CD44$^+$/CD24$^-$ cells) that were isolated by FACS were found to be enriched for P-RSK$^{S221/227}$ and P-YB-1^{S102} compared to CD44$^-$/CD24$^+$ cells suggesting that this pathway may be particularly important in CD44$^+$/CD24$^-$ cells (Fig. 5A, 5B). These TICs were dependent upon RSK signaling because exposing them to BI-D1870 reduced cell growth by >90% after 72 hours at doses as low as 1 μM (Fig. 5C). Apoptosis was also induced as indicated by increased PI uptake (Fig. 5D). When compared with their

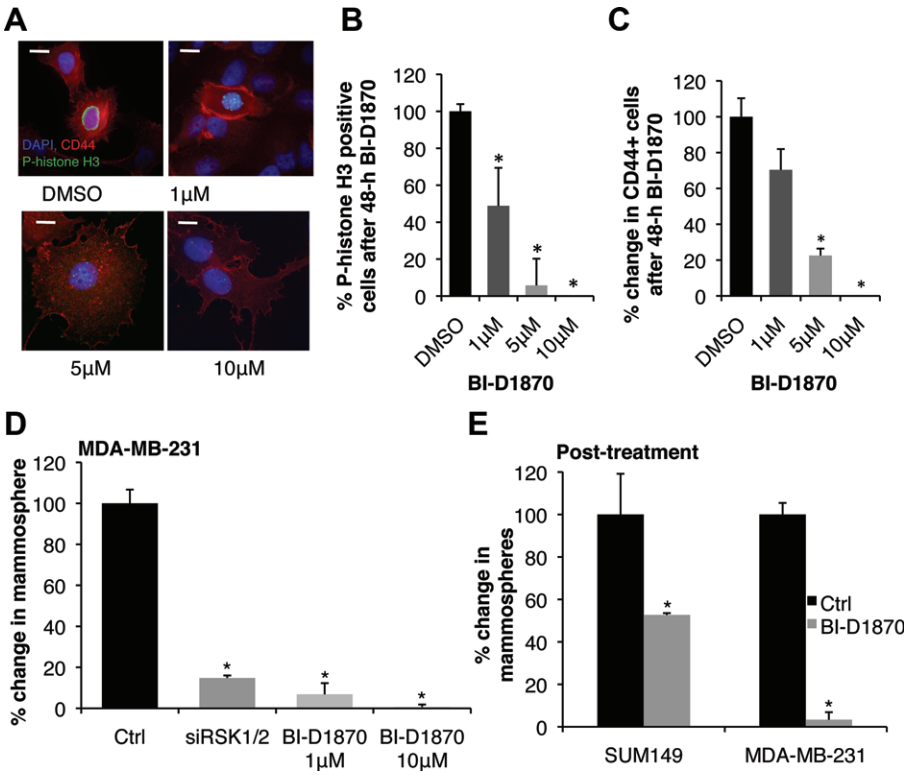

Figure 4. Targeting RSK suppresses growth of tumor-initiating cells. **(A):** $CD44^+$ cells express high levels of P-histone $H3^{S10}$. Immunofluorescence staining shows CD44 (red), P-histone H3 (green), and hoechst (blue). Scale bar = 15 μm. **(B,C):** Treatment with BI-D1870 (1-10 μM) reduces P-histone $H3^{S10}$ and CD44 protein levels, respectively. **(D):** MDA-MB-231 cells treated with BI-D1870 or RSK1/2 small interfering RNA had a significantly reduced ability to form mammospheres after 7 days. **(E):** Mammosphere number was reduced following treatment of established spheres with BI-D1870 (10 μM). Abbreviations: DMSO, dimethyl sulphoxide; RSK, ribosomal S6 kinase. *$p < 0.05$.

$CD44^-/CD24^+$ counterparts, TICs were found to have increased PI uptake after treatment with BI-D1870; perhaps, due to increased RSK expression in this population (Supporting Information Fig. S5D). Knockdown of RSK2 expression using siRNA similarly decreased growth and induced apoptosis in $CD44^+/CD24^-$ cells (Fig. 5E, 5F, respectively). In parallel with our findings in unsorted cells, RSK2 inhibition was more effective at suppressing growth and inducing apoptosis in TICs than RSK1 inhibition. The studies thus far indicate that RSK2 inhibitors are exciting therapeutic leads for inhibiting TICs.

One important consideration is the effect of inhibiting RSK on normal stem cells. To address this question, we assessed the growth and differentiation of primary human hematopoietic stem cells when dosed with a range (0.015–15 μM) of BI-D1870. Treatment with BI-D1870 did not suppress the growth or differentiation of normal human hematopoietic stem cells (at doses <5μM, Supporting Information Table S2, Fig. S6A, S6B). We subsequently investigated the effect of inhibiting RSK on normal breast epithelial cells (184htert). In accordance with the data on the hematopoietic stem cells, we observed no effect on the growth of 184htert cells at concentrations up to 2 μM BI-D1870, a dose that suppressed growth of TICs by 90% (Supporting Information Fig. S7A). Interestingly, neither SL0101 (50 μM) or RSK siRNA, in particular RSK2 siRNA, had any effect on growth of normal mammary epithelial 184htert cells (Supporting Information Fig. S7B, S7C, respectively).

RSK Inhibition Delays Tumor Initiation

To directly assess the effects of RSK knockdown on tumor formation, we performed a transient RSK2 knockdown in MDA-MB-231 cells that homogeneously express high CD44 and low CD24 (Fig. 6A). RSK2 was silenced for 48 hours and loss of expression was confirmed by qRT-PCR and immunoblotting (Fig. 6B). We observed >80% decrease in RSK2 expression (Fig. 6B). This decrease in RSK leads to a subsequent loss of CD44 protein expression (Supporting Information Fig. S8A). NOD/SCID mice were injected with MDA-MB-231 cells transfected with either the scrambled control siRNA or RSK2 siRNA (1×10^6 cells per MFP). Given the short half-life of siRNAs (10 days; Supporting Information Fig. S8B, S8C), high cell numbers were required. Based on our prior experience, we knew that this number of cells would initiate tumor formation within approximately 2 weeks and that the siRNAs would still be active within this timeframe. It was interesting to find that 100% of the mice (4/4) that received the MDA-MB-231 cells exposed to the scrambled control developed palpable tumors beginning at 17 days postinjection. In contrast, only 40% of the mice (2/5) developed tumors following RSK2 inhibition at the same time interval, and this trend continued out until 24 days postinjection (Fig. 6C). The delay in tumor initiation correlated with RSK2 expression in that after 3 weeks all the mice eventually developed tumors (day 27) (Fig. 6C). At this point, we validated RSK2 expression in all tumors and it was found to be equal to the controls (Supporting Information Fig. S8D). Once RSK2 was re-expressed, tumors grew at equivalent rates; however, the average size of the RSK2 siRNA tumors was approximately half that of the control tumors (Supporting Information Table S3). This is the first proof-of-concept study to show that RSK inhibitors block the growth of TNBC cells in vitro and in vivo in part through the loss of TICs.

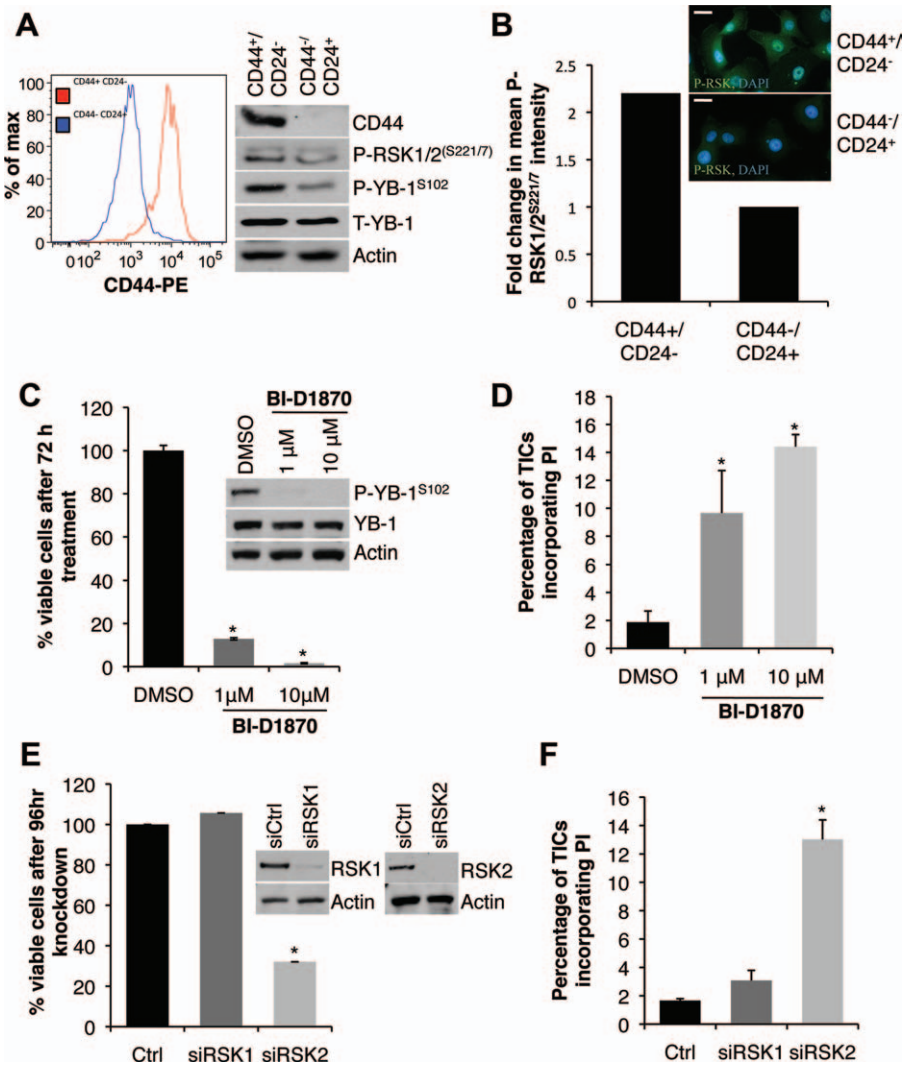

Figure 5. Inhibiting RSK suppresses growth in $CD44^+$ cells. **(A):** $CD44^+/CD24^-$ sorted cells have a much higher level of activated RSK and YB-1 than $CD44^-/CD24^+$ cells. **(B):** Quantification of the level of P-$RSK^{S221/7}$ in $CD44^+$ compared to $CD44^-$ cells along with representative images of P-$RSK^{S221/7}$ staining. **(C):** Treatment of $CD44^+/CD24^-$ sorted cells with a single dose of BI-D1870 (1–10 μM) results in a ~90% decrease in growth after 72 hours. **(D):** Treatment of $CD44^+/CD24^-$ sorted cells with BI-D1870 induces apoptosis in TICs as indicated by PI uptake. **(E):** Knockdown of RSK2 in $CD44^+/CD24^-$ sorted SUM149 cells resulted in a ~70% decrease in growth after 96 hours. Western blot demonstrates loss of protein. **(F):** Suppression of RSK2 with siRNA led to an increase in apoptosis as demonstrated by elevated PI uptake. Abbreviations: DMSO, dimethyl sulphoxide; PI, propidium iodide; RSK, ribosomal S6 kinase; TIC, tumor-initiating cell; YB-1, Y-box binding protein-1. *$p < 0.05$.

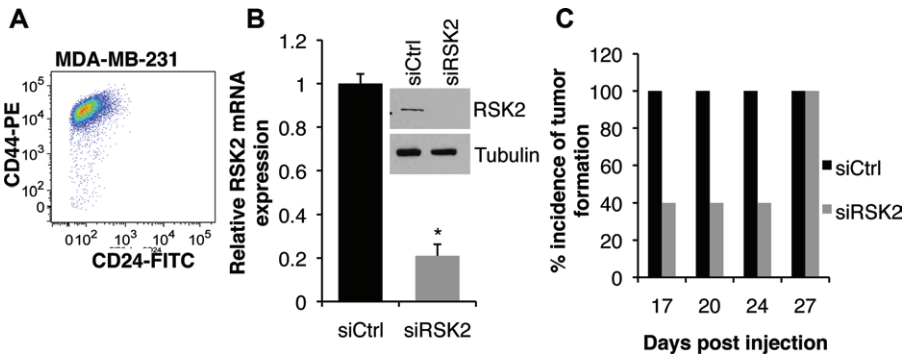

Figure 6. Inhibiting RSK2 delays tumor initiation. **(A):** MDA-MB-231 cells are ubiquitously $CD44^+/CD24^-$ as demonstrated by flow cytometry, and these cells form tumors in mice within 2 weeks (data not shown). **(B):** A reduction in RSK2 transcript and protein (inset) was achieved at 48 hours in MDA-MB-231 cells. **(C):** Transient RSK2 knockdown inhibited tumor initiation of MDA-MB-231 cells (1×10^6 cells per injection) in nonobese diabetic/severe combined immunodeficient mice ($p = .058$). Abbreviation: RSK, ribosomal S6 kinase. *$p < 0.05$.

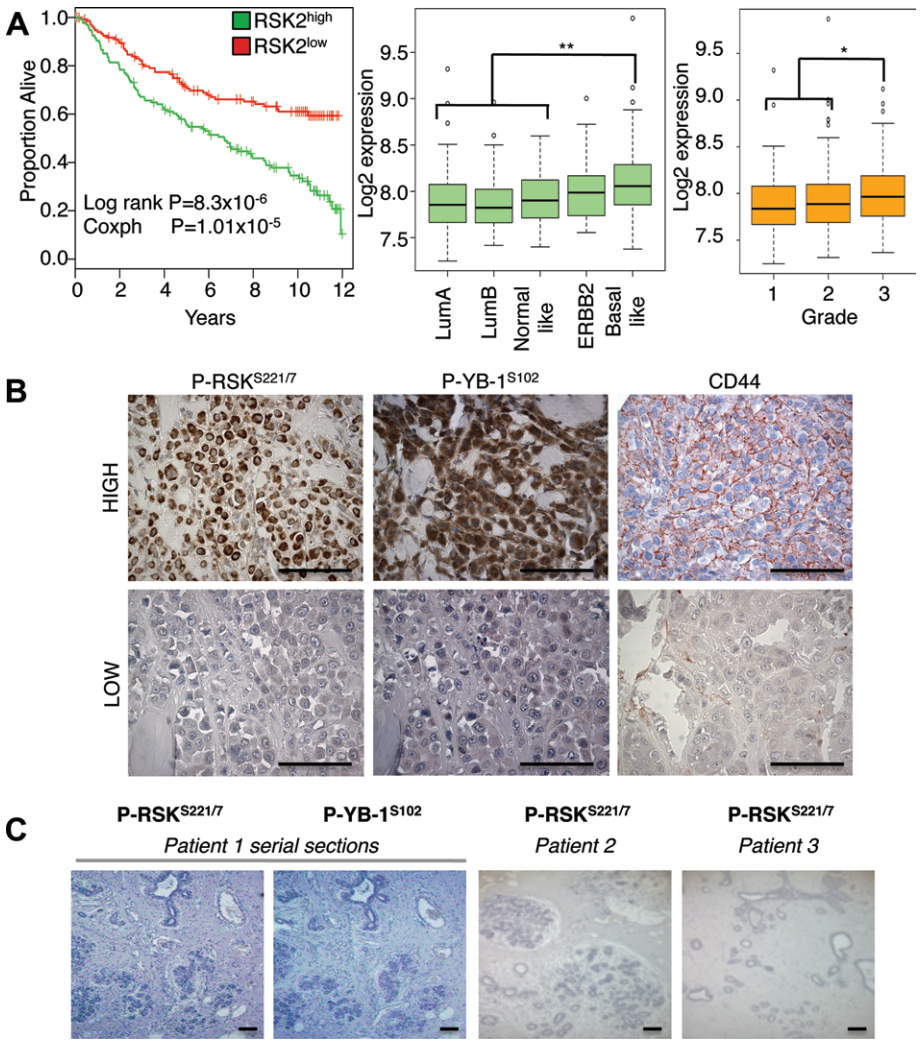

Figure 7. Activated RSK is expressed in triple-negative breast cancer patient samples. **(A):** RSK2 mRNA was associated with poor survival in 244 breast cancer cases who had not received chemotherapy (log-rank $p = 8.3 \times 10^{-6}$; Cox proportional hazards $p = 1 \times 10^{-5}$) (left). When examining RSK2 expression in a cohort of 771 breast cancer cases representing all subtypes, it was highest in the basal-like subtype (center) ($n = 771$; $p < .005$) and in those of high-grade (right) ($n = 771$; $p < .05$). **(B):** P-RSK$^{S221/7}$ was detected in 13/18 aggressive breast tumor samples. P-YB-1^{S102} and CD44 expression also correlated (Supporting Information Tables). **(C):** Expression of activated RSK and YB-1 was not detected in normal breast tissue. Scale bars = 100 μm. Abbreviations: RSK, ribosomal S6 kinase; YB-1, Y-box binding protein-1. $^*p < 0.05$, $^{**}p < 0.005$.

Activated RSK Is Expressed in Patient Samples

As we found RSK2 to have the most significant effect on TNBC and TIC survival, we then investigated whether it was also important in patient samples. We assessed RSK2 mRNA levels in 244 breast cancer patients who had not received adjuvant therapy. Patients with high RSK2 expression had significantly worse survival outcomes (log-rank test $p = 8.3 \times 10^{-6}$; Cox proportional hazards $p = 1.01 \times 10^{-5}$) (Fig. 7A left). Analysis of the entire cohort of 771 patients showed that interestingly, RSK2 expression was highest in tumors of the basal-like subtype (Fig. 7A center) and in those with the highest grade (grade 3; Fig. 7A right). In support of this data, we demonstrated that RSK2 expression levels were consistently significantly higher in TNBC cell lines compared with non-TNBC cell lines (Supporting Information Fig. S9). It is important to note that while the basal-like subtype is defined by gene expression, the majority of basal-like breast cancers are also triple negative in terms of expression of cell surface receptor proteins [38].

Finally, we obtained a focused collection of 18 high-grade breast cancers to address whether RSK was active in TNBC and whether it correlated with either P-YB-1^{S102} or CD44. P-RSK$^{S221/227}$ was highly expressed in 85% (11/13) of TNBC (Fig. 7B). Activated RSK significantly correlated with P-YB-1^{S102} ($p = .0002$, Spearman's correlation 0.771) (Supporting Information Table S4). Furthermore, in more than half the cases, CD44 expression tracks with P-RSK$^{S221/227}$ and P-YB-1^{S102} ($p = .0333$, Spearman's correlation 0.5031, and $p = .0109$, Spearman's correlation 0.5840, respectively) (Supporting Information Table S4). In contrast to the high frequency of RSK and YB-1 activation in TNBC, P-RSK$^{S221/227}$ and P-YB-1^{S102} were not expressed in primary normal mammary ducts (Fig. 7C). To expand this finding, 10 additional normal breast tissues were examined and RSK was consistently not expressed (Fig. 7C, two examples shown). We thus conclude that the RSK/YB-1/CD44 pathway is activated in primary TNBC.

Discussion

Currently, the treatment of TNBC is limited to conventional chemotherapy as targeted therapies are not available. YB-1 is a signature feature of highly aggressive breast cancers, such as TNBC, and is associated with poor clinical outcome and disease relapse [39]. It is possible that this is in part, due to the high proportion of TICs in TNBC. YB-1 is an early driver in breast cancer formation and evokes cancer susceptibility by promoting genetic instability leading to tumorigenesis [40]. We have previously demonstrated YB-1 as a critical regulator of drug resistance and TIC phenotype in breast cancer [11]. In the brain, YB-1 overexpression promotes expression of stem-cell genes and prevents differentiation of both normal neural stem cells and also brain TICs [41]. Furthermore, YB-1 promotes castration-resistant prostate cancer cell growth, thus its influence in drug-resistant cell populations extends beyond breast cancer [42]. However, the lack of molecular therapies specific to YB-1 limits the ability to target it directly.

Herein, we have identified that targeting RSK is a novel strategy for specifically inhibiting growth of TNBC but not normal breast epithelial cells. These findings are consistent with those observed by Smith et al. in an ER-positive model, MCF-7 cells, where growth suppression was demonstrated following treatment with SL0101 [30]. Immortalized normal breast cells, MCF-10A cells were also not effected. In this study, they did not assess the effects of targeting RSK using a model of TNBC. It is noteworthy that the TNBC models that we assessed were exquisitely sensitive to RSK inhibition, more so than that reported for MCF-7 cells [30]. For example, Smith et al. reported that loss of RSK1 or RSK2 suppressed tumor cell growth by ~40% [30]. Yet we show that the growth of TNBC cells is inhibited by 90%–100% when RSK is inhibited with RSK2 siRNA, SL0101, or BI-D1870. Importantly, upon subsequent treatments with BI-D1870, cells do not acquire resistance to the compound. Currently, this represents the most striking effect of a kinase inhibitor on TNBC growth.

TNBCs have a higher percentage of TICs—as defined by CD44 expression—compared to other breast cancer subtypes, which could partially account for their increased propensity to relapse [6]. The growth of the $CD44^+$ cells is notably different in that the number of mitotic figures and the levels of P-histone $H3^{S10}$ are considerably higher in those cells compared to the $CD44^-$ cells. One way of explaining this growth advantage is through the activation of signaling in CD44-positive cells is by way of an autocrine loop where its ligand hyaluronan is produced. The MDA-MB-231 cells are described as having an autocrine production of hyaluronan that activates cell signaling through recruitment of Rhamm and Erk, this in turn would engage the mitogen activated protein kinase (MAPK) pathway [43]. Consistent with this model, the MEK1 inhibitor PD098059 disrupts this pathway. While the authors attribute the CD44/Rhamm/Erk pathway to increased cell motility, which is of course an important aspect of the spread of TICs from the primary site this signaling network would also fuel cellular proliferation and drug resistance. While CD44 is used as a means to isolate TICs, it too serves important functions in maintaining cell growth and invasion. Thus, eliminating the TIC subpopulation alongside the rest of the tumor may help overcome the challenge of relapse.

We previously identified the RSK downstream target YB-1 as a critical regulator of a TIC phenotype [11]. Knockdown of YB-1 using siRNA in TNBC resulted in decreased growth and mammosphere formation [11]. Herein, we demonstrate that inhibiting RSK, particularly RSK2, is sufficient to suppress growth in the $CD44^+CD24^-$ population within TNBC. Additionally, the ability to suppress mammosphere formation indicates an inhibition of self-renewal. One major challenge in the development of TIC-directed therapies is that many of the critical signaling pathways in TICs are also crucial for normal stem cell survival. Thus, inhibiting these pathways could result in severe toxicity to normal stem cells. We found that RSK inhibition demonstrated specific/increased toxicity to breast TICs when compared with normal hematopoietic stem cells. This is in line with a study by Kang et al., which showed that loss of RSK2 via knockout also had no affect on the hematopoietic stem cell subpopulation [44]. Collectively, these data indicate that RSK inhibition is effective at eliminating breast cancer TICs but unlike conventional chemotherapies has little effect on normal stem cells. We conclude that RSK is uniquely linked to promote the proliferation of $CD44^+$ cells, and as such targeting this pathway has important implications in the management of TNBC. Furthermore, CD44 is a cancer stem cell biomarker for many other types of cancer including leukemia [45], prostate [46], pancreatic [47], and colon [48]. Therefore, we propose that RSK inhibitors may be used to inhibit the growth of cancer stem cells from a wide range of tumor types.

RSK2 has therefore become a subject of interest as an emerging therapeutic target [49]. In part, this is because RSK2 has been linked to numerous cancer types [50] such as head and neck squamous cell carcinoma [50] and those of hematopoietic origin [20]. More recently, a study to determine therapeutic targets for specific breast cancer subtypes by a siRNA screen identified RSK2 as one of three genes with potential for the TNBC subtype [31]. Taken together with our data we have identified RSK2 as a promising therapeutic target for TNBC.

Conclusion

Our exciting and timely breakthrough brings forth RSK, and RSK2 in particular, as a druggable molecular target for TNBC. Moreover, RSK inhibitors have the highly desirable property of inhibiting TICs, and given this it stands out as a cutting-edge opportunity to potentially improve the treatment of TNBC.

Acknowledgments

Thank you to James Chen for carrying out the statistical analysis for the tumor tissue microarray staining. We acknowledge NHS funding to the RMH NIHR Biomedical Research Centre. Grants are from Canadian Breast Cancer Foundation (AS), Canadian Institutes of Health Research (SED), Child and Family Research Institute (KR), New Zealand Breast Cancer Research Trust, Cancer Society of New Zealand (CP, AL), and American Association for Cancer Research as part of the Stand Up to Cancer Breast Cancer Dream Team Initiative (RB, JF, CL, AA).

Disclosure of Potential Conflicts of Interest

There are no conflicts of interest.

REFERENCES

1 Dent R, Trudeau M, Pritchard KI et al. Triple-negative breast cancer: Clinical features and patterns of recurrence. Clin Cancer Res 2007;13: 4429–4434.
2 Liedtke C, Mazouni C, Hess KR et al. Response to neoadjuvant therapy and long-term survival in patients with triple-negative breast cancer. J Clin Oncol 2008;26:1275–1281.
3 Honeth G, Bendahl PO, Ringnér M et al. The CD44+/CD24- phenotype is enriched in basal-like breast tumors. Breast Cancer Res 2008;10:R53.
4 Charafe-Jauffret E, Ginestier C, Iovino F et al. Breast cancer cell lines contain functional cancer stem cells with metastatic capacity and a distinct molecular signature. Cancer Res 2009;69:1302–1313.
5 Nakshatri H, Srour EF, Badve S. Breast cancer stem cells and intrinsic subtypes: Controversies rage on. Curr Stem Cell Res Ther 2009;4: 50–60.
6 Park SY, Lee HE, Li H et al. Heterogeneity for stem cell-related markers according to tumor subtype and histologic stage in breast cancer. Clin Cancer Res 2010;16:876–887.
7 Creighton CJ, Li X, Landis M et al. Residual breast cancers after conventional therapy display mesenchymal as well as tumor-initiating features. Proc Natl Acad Sci USA 2009;106:13820–13825.
8 Li X, Lewis MT, Huang J et al. Intrinsic resistance of tumorigenic breast cancer cells to chemotherapy. J Natl Cancer Inst 2008;100: 672–679.
9 Phillips TM, McBride WH, Pajonk F. The response of CD24-/low/ CD44+ breast cancer-initiating cells to radiation. J Natl Cancer Inst 2006;98:1777–1785.
10 Fillmore CM, Kuperwasser C. Human breast cancer cell lines contain stem-like cells that self-renew, give rise to phenotypically diverse progeny and survive chemotherapy. Breast Cancer Res 2008; 10:R25.
11 To K, Fotovati A, Reipas KM et al. YB-1 induces expression of CD44 and CD49f leading to enhanced self-renewal, mammosphere growth, and drug resistance. Cancer Res 2010;70:2840–2851.
12 Stratford AL, Reipas K, Maxwell C et al. Targeting tumour-initiating cells to improve the cure rates for triple-negative breast cancer. Expert Rev Mol Med 2010;12:e22.
13 Dontu G, Wicha MS. Survival of mammary stem cells in suspension culture: Implications for stem cell biology and neoplasia. J Mammary Gland Biol Neoplasia 2005;10:75–86.
14 Ponti D, Costa A, Zaffaroni N et al. Isolation and in vitro propagation of tumorigenic breast cancer cells with stem/progenitor cell properties. Cancer Res 2005;65:5506–5511.
15 Murohashi M, Hinohara K, Kuroda M et al. Gene set enrichment analysis provides insight into novel signalling pathways in breast cancer stem cells. Br J Cancer 2010;102:206–212.
16 Blick T, Hugo H, Widodo E et al. Epithelial mesenchymal transition traits in human breast cancer cell lines parallel the CD44(hi/)CD24 (lo/-) stem cell phenotype in human breast cancer. J Mammary Gland Biol Neoplasia 2010;15:235–252.
17 Shipitsin M, Campbell LL, Argani P et al. Molecular definition of breast tumor heterogeneity. Cancer Cell 2007;11:259–273.
18 Sawyers CL. Lessons learned from the development of kinase inhibitors. Clin Adv Hematol Oncol 2009;7:588–589.
19 Carriere A, Ray H, Blenis J et al. The RSK factors of activating the Ras/MAPK signaling cascade. Front Biosci 2008;13:4258–4275.
20 Kang S, Dong S, Gu TL et al. FGFR3 activates RSK2 to mediate hematopoietic transformation through tyrosine phosphorylation of RSK2 and activation of the MEK/ERK pathway. Cancer Cell 2007;12: 201–214.
21 Law JH, Habibi G, Hu K et al. Phosphorylated insulin-like growth factor-1/insulin receptor is present in all breast cancersubtypes and is related to poor survival. Cancer Res 2008;68:10238–10246.
22 Stratford AL, Fry CJ, Desilets C et al. Y-box binding protein-1 serine 102 is a downstream target of p90 ribosomal S6 kinase in basal-like breast cancer cells. Breast Cancer Res 2008;10:R99.
23 Anjum R, Blenis J. The RSK family of kinases: Emerging roles in cellular signalling. Nat Rev Mol Cell Biol 2008;9:747–758.
24 Chen R-H, Abate C, Blenis J. Phosphorylation of the c-Fos transrepression domain by mitogen-activated protein kinase and 90-kDa ribosomal S6 kinase. Proc Natl Acad Sci USA 1993;90:10952–10956.
25 Shimamura A, Ballif BA, Richards SA et al. Rsk1 mediates a MEK-MAP kinase cell survival signal. Curr Biol 2000;10:127–135.
26 Sutherland C, Leighton IA, Cohen P. Inactivation of glycogen synthase kinase-3 β by phosphorylation: New kinase connections in insulin and growth-factor signalling. Biochem J 1993;296:15–19.
27 Lau PNL, Cheung P. Histone code pathway involving H3 S28 phosphorylation and K27 acetylation activates transcription and antagonizes polycomb silencing. Proc Natl Acad Sci USA 2011;108: 2801–2806.
28 Sassone-Corsi P, Mizzen CA, Cheung P et al. Requirement of RSK2 for epidermal growth factor-activated phosphorylation of histone H3. Science 1999;285:886–891.
29 To K, Zhao Y, Jiang H et al. The phosphoinositide-dependent kinase-1 inhibitor, OSU03012, prevents Y-box binding protein-1 (YB-1) from inducing epidermal growth factor receptor (EGFR). Mol Pharmacol 2007;72:641–652.
30 Smith JA, Poteet-Smith CE, Xu Y et al. Identification of the first specific inhibitor of p90 ribosomal S6 kinase (RSK) reveals an unexpected role for RSK in cancer cell proliferation. Cancer Res 2005;65: 1027–1034.
31 Brough R, Frankum JR, Sims D et al. Functional viability profiles of breast cancer. Cancer Discov 2011;1:260–273.
32 Wu J, Lee C, Yokom D et al. Disruption of the Y-Box binding protein-1 results in suppression of the epidermal growth factor receptor and HER-2. Cancer Res 2006;66:4872–4879.
33 Lasham A, Samuel W, Cao H et al. YB-1, the E2F pathway, and regulation of tumor cell growth. J Natl Cancer Inst 2012;104:1–14.
34 Harrington DP, Fleming TR. A class of rank test procedures for censored survival data. Biometrika 1982;69:553–566.
35 Desmedt C, Piette F, Loi S et al. Strong time dependence of the 76-gene prognostic signature for node-negative breast cancer patients in the TRANSBIG multicenter independent validation series. Clin Cancer Res 2007;13:3207–3214.
36 Law JH, Li Y, To K et al. Molecular decoy to the Y-box binding protein-1 suppresses the growth of breast and prostate cancer cells whilst sparing normal cell viability. PLoS One 2010;5:e12661.
37 Calcagno AM, Salcido CD, Gillet J-P et al. Prolonged drug selection of breast cancer cells and enrichment of cancer stem cell characteristics. J Natl Cancer Inst 2010;102:1637–1652.
38 Foulkes WD, Smith IE, Reis-Filho JS. Triple-negative breast cancer. N Engl J Med 2010;363:1938–1948.
39 Habibi G, Leung S, Law JH et al. Re-defining prognostic factors for breast cancer: YB-1 is a stronger predictor of relapse and disease specific survival than estrogen receptor or HER-2 across all tumor subtypes. Breast Cancer Res 2008;10:R86.
40 Davies AH, Barrett I, Pambid MR et al. YB-1 evokes susceptibility to cancer through cytokinesis failure, mitotic dysfunction and HER2 amplification. Oncogene 2011;30:3649–3660.
41 Fotovati A, Abu-Ali S, Wang PS et al. YB-1 bridges neural stem cells and brain-tumor initiating cells via its roles in differentiation and cell growth. Cancer Res 2011;71:5569–5578.
42 Shiota M, Takeuchi A, Song Y et al. Y-box binding protein-1 promotes castration-resistant prostate cancer growth via androgen receptor expression. Endocr Relat Cancer 2011;18:505–517.
43 Hamilton SR, Fard SF, Paiwand FF et al. The hyaluronan receptors CD44 and Rhamm (CD168) form complexes with ERK1,2 that sustain high basal motility in breast cancer cells. J Biol Chem 2007;282: 16667–16680.
44 Kang S, Elf S, Dong S et al. Fibroblast growth factor receptor 3 associates with and tyrosine phosphorylates p90 RSK2, leading to RSK2 activation that mediates hematopoietic transformation. Mol Cell Biol 2009;29:2105–2117.
45 Jin L, Hope KJ, Zhai Q et al. Targeting of CD44 eradicates human acute myeloid leukemic stem cells. Nat Med 2006;12:1167–1174.
46 Patrawala L, Calhoun-Davis T, Schneider-Broussard R et al. Hierarchical organization of prostate cancer cells in xenograft tumors: The CD44+alpha2beta1+ cell population is enriched in tumor-initiating cells. Cancer Res 2007;67:8973.
47 Li C, Heidt DG, Dalerba P et al. Identification of pancreatic cancer stem cells. Cancer Res 2007;67:1030–1037.
48 Dalerba P, Dylla SJ, Park IK et al. Phenotypic characterization of human colorectal cancer stem cells. Proc Natl Acad Sci USA 2007; 104:10158–10163.
49 Stratford AL, Dunn SE. The promise and challenges of targeting RSK for the treatment of cancer. Expert Opin Ther Targets 2011;15:1–4.
50 Kang S, Elf S, Lythgoe K et al. p90 ribosomal S6 kinase 2 promotes invasion and metastasis of human head and neck squamous cell carcinoma cells. J Clin Invest 2010;120:1165–1177.


See www.StemCells.com for supporting information available online.